



OPEN

SUBJECT AREAS:

SERS

PHOTOCATALYSIS

CATALYTIC MECHANISMS

RAMAN SPECTROSCOPY

# Mechanistic understanding of surface plasmon assisted catalysis on a single particle: cyclic redox of 4-aminothiophenol

Ping Xu<sup>1,2</sup>, Leilei Kang<sup>1</sup>, Nathan H. Mack<sup>2</sup>, Kirk S. Schanze<sup>3</sup>, Xijiang Han<sup>1</sup> & Hsing-Lin Wang<sup>2</sup>Received  
3 June 2013Accepted  
2 October 2013Published  
21 October 2013

Correspondence and requests for materials should be addressed to P.X. (pxu@hit.edu.cn); X.J.H. (hanxijiang@hit.edu.cn) or H.-L.W. (hwang@lanl.gov)

<sup>1</sup>Department of Chemistry, Harbin Institute of Technology, Harbin 150001, People's Republic of China, <sup>2</sup>Chemistry Division, Physical Chemistry and Applied Spectroscopy, Los Alamos National Laboratory, Los Alamos, NM 87545, United States of America, <sup>3</sup>Department of Chemistry, University of Florida, Gainesville, FL 32611, United States of America.

Surface plasmon assisted catalysis (SPAC) reactions of 4-aminothiophenol (4ATP) to and back from 4,4'-dimercaptoazobenzene (DMAB) have been investigated by single particle surface enhanced Raman spectroscopy, using a self-designed gas flow cell to control the reductive/oxidative environment over the reactions. Conversion of 4ATP into DMAB is induced by energy transfer (plasmonic heating) from surface plasmon resonance to 4ATP, where O<sub>2</sub> (as an electron acceptor) is essential and H<sub>2</sub>O (as a base) can accelerate the reaction. In contrast, hot electron (from surface plasmon decay) induction drives the reverse reaction of DMAB to 4ATP, where H<sub>2</sub>O (or H<sub>2</sub>) acts as the hydrogen source. More interestingly, the cyclic redox between 4ATP and DMAB by SPAC approach has been demonstrated. This SPAC methodology presents a unique platform for studying chemical reactions that are not possible under standard synthetic conditions.

Surface plasmon assisted catalysis (SPAC) has shown promise as a novel pathway for studying chemical reactions on plasmonic metal nanostructures, typically with the assistance of surface enhanced Raman spectroscopy (SERS) or tip enhanced Raman spectroscopy (TERS) techniques<sup>1,2</sup>. SERS and TERS not only induce chemical reactions at a metal surface through surface plasmon resonance, they also act as sensitive spectroscopic probes for monitoring the structural change of the adsorbed reactants<sup>3,4</sup>. SPAC reactions were first discovered on 4-aminothiophenol (4ATP) using SERS, where 4ATP was observed to gradually convert (dimerize) to 4,4'-dimercaptoazobenzene (DMAB) upon continuous laser excitation<sup>2,5–10</sup>. Recently, 4-nitrothiophenol (4NTP) has also been shown to dimerize into DMAB by this direct surface plasmon assisted technique<sup>11–13</sup>. Hot electrons generated during surface plasmon excitation are regarded as the species that mediate the conversion of 4NTP into DMAB through an electron transfer process<sup>11,12</sup>, which is chemically a reduction reaction<sup>14,15</sup>. However, SPAC conversion of 4ATP into DMAB is an oxidation reaction, where electron loss from 4ATP to either metal surface or local environment leads to the formation of DMAB. Such a reaction is complex, involving transfer of multiple electrons and protons, and the underlying mechanism of the SPAC-based oxidation reaction has not been clearly understood.

Herein, we demonstrate careful monitoring of the SPAC reaction of 4ATP and DMAB using a home-made gas flow cell (Fig. 1a), which allows precise control of the reaction atmosphere. Time-dependent SERS spectra were recorded on a single silver microsphere (~1.5 μm in size) with hierarchical nanostructures (Fig. 1b), prepared from our acid directed synthetic route (see experimental details in Supplemental Information)<sup>13,16</sup>. This experimental set-up has the advantage of confining the reactions within a limited area that can be completely illuminated within the focused laser spot size. The size feature of the Ag particles allows easy location of one single particle under optical microscope (Fig. S1), and the hierarchical nanoscaled surface features (assembled by very thin nanosheets) warrant the surface roughness and generation of strong surface plasmon resonance under laser excitation. As the laser needs to pass through the window (an ultrathin glass slide) of the reaction station and focus on one single Ag particle on the silicon wafer (Fig. 1c), the distance between the raised stage at the bottom part and the window at the top part should be carefully controlled. This technique, combining the gas flow cell and

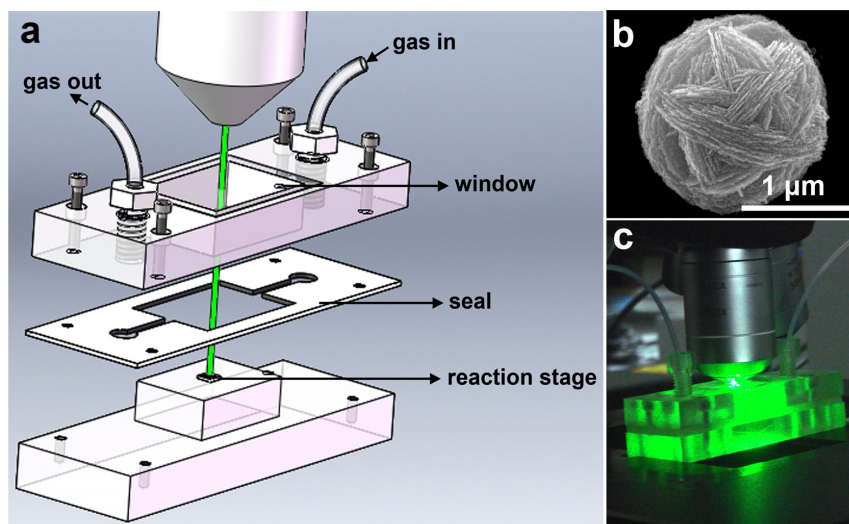


**Figure 1** | Schematic illustration of the experimental set-up. (a), Structure schematic of the gas flow cell for monitoring the surface plasmon assisted catalysis (SPAC) reaction under controlled gas atmosphere. (b), SEM image of a single Ag microsphere used for the single particle SERS technique. (c), A photo shows monitoring the SPAC reaction using our designed reaction station.

single particle SERS, provides a facile and unique method to study SPAC reactions under controlled atmosphere and monitor the reaction in a confined space, which is not easily accessible by conventional synthesis routes.

## Results

In order to eliminate the possible influence of the as-fabricated device on the SPAC reaction, a control experiment was conducted by recording the time-dependent SERS spectra of 4ATP inside and outside of the reaction station without gas purging. The reaction rates of 4ATP converting into DMAB are almost identical under both conditions (completion in 5 min as indicated by a leveling off in intensities of DMAB bands) (Fig. S2), indicating no interference from the experimental apparatus and establishing a baseline reaction rate to compare with other reactions under controlled atmospheres. Elimination of the influence of the apparatus renders us a unique opportunity to study the underlying mechanisms of the SPAC oxidation reaction of 4ATP to DMAB by performing the experiments under a controlled gas atmosphere. For example, when the reaction is carried out under  $N_2$ , all other experimental parameters being the same, 4ATP does not dimerize into DMAB, regardless of the laser excitation wavelength (533 nm or 632 nm) (Fig. S3). This result suggests that some gas component(s) in the air, whether  $O_2$  or  $H_2O$ , must be involved in the plasmon-driven conversion of 4ATP into DMAB. This result also implies that it is not the hot electrons generated through surface plasmon excitation that induce the dimerization of 4ATP, as  $N_2$  gas inside the reaction station should not quench the generation of surface plasmons.

Considering the oxidative nature of 4ATP dimerization, similar data were taken under an  $O_2$  atmosphere. Here, using a 532 nm laser at a power of 0.05 mW caused the reaction to proceed too fast ( $\leq 1$  min) to capture the spectroscopic changes by SERS. Therefore, a 633 nm laser (0.05 mW) was used to better record the reaction process. Though these Ag microspheres only display a broad extinction feature in the range of 400–700 nm with  $\lambda_{max}$  at  $\sim 465$  nm (Fig. S4), our previous study has shown a wavelength-dependence on the SPAC reaction of converting 4-NTP to DMAB<sup>13</sup>, with 532 nm excitation being significantly faster than 633 nm laser excitation, given the same laser power. Actually, theoretical simulations have also confirmed that the electromagnetic enhancement at the surface of Ag materials with an incident wavelength of 532 nm or 514.5 nm is much stronger than that using 633 nm<sup>17</sup>. As shown in Fig. 2 a and

b, conversion of 4ATP into DMAB can be clearly distinguished from the new Raman bands that appear at  $1140\text{ cm}^{-1}$  due to  $\beta(\text{CH})$ , and  $1390$  and  $1432\text{ cm}^{-1}$  due to  $\nu(\text{N}=\text{N})$ <sup>18</sup>. The reaction will be terminated at a point when no obvious intensity changes of the DMAB Raman bands are observed. Notably, increasing the laser power from 0.05 mW to 0.2 mW results in another Raman band ascribed to the  $\nu(\text{NO}_2)$  at  $1335\text{ cm}^{-1}$ , concomitant with the production of DMAB (Fig. 2 c and d). This result indicates that given sufficient laser power and higher concentration of  $O_2$  (as compared to ambient air), 4ATP can simultaneously be converted to 4NTP and DMAB, a strong implication that  $O_2$  is involved in the reaction. In the above experiment,  $O_2$  plays two separate roles: serving as 1) an electron acceptor in the oxidative dimerization of 4ATP to DMAB; and 2) an oxidant and O-atom source in the oxidation of 4ATP to 4NTP. Conversion of 4ATP to 4NTP by direct laser excitation has not been observed in previous SPAC reaction studies of 4ATP at ambient conditions<sup>2,5-9</sup>. Additionally, the produced 4NTP cannot be converted to DMAB as seen using 4NTP as the starting material<sup>11-13</sup>, most likely due to inhibition of the reductive dimerization by the presence of  $O_2$ . The significantly reduced reaction rate of 4ATP to DMAB under an  $O_2$  atmosphere as compared to that in air (>15 min vs. <5 min) and non-reactivity under  $N_2$  indicate that an additional component, most likely moisture vapor ( $H_2O$ ) in air, is involved in the overall dimerization. To validate this hypothesis, a stream of moisture saturated  $N_2$  gas (all  $O_2$  eliminated from the reaction vessel) was flowed over the sample. Surprisingly, no reaction occurred when the system was confined in a  $N_2$  saturated  $H_2O$  vapor environment (Fig. S5), again implying that  $O_2$ , as an oxidizing agent, is required to convert 4ATP into DMAB. A subsequent control experiment using  $H_2O$  moisture saturated  $O_2$  as the carrier gas results in an extremely fast conversion (within 3 min) (Fig. S6), clearly demonstrating that not only is the SPAC reaction of 4ATP into DMAB dependent on optical excitation, but also that  $O_2$  and  $H_2O$  play defining roles in the rate limiting steps of the reaction ( $O_2$  is indispensable as an oxidant, while  $H_2O$  plays a role to facilitate the reaction). Moreover, the non-reactivity of 4ATP under  $N_2$  atmosphere interprets that the appearance of the Raman bands at  $1390$  and  $1432\text{ cm}^{-1}$  should be due to the conversion of 4ATP to DMAB, but not from chemical enhancement of 4ATP<sup>19</sup>.

These data, taken together, strongly suggest reaction mechanisms for the reaction of 4ATP to DMAB that are not dependent on hot electrons from surface plasmon decay, but a thermal mechanism caused by enhanced surface plasmon resonance absorption at the

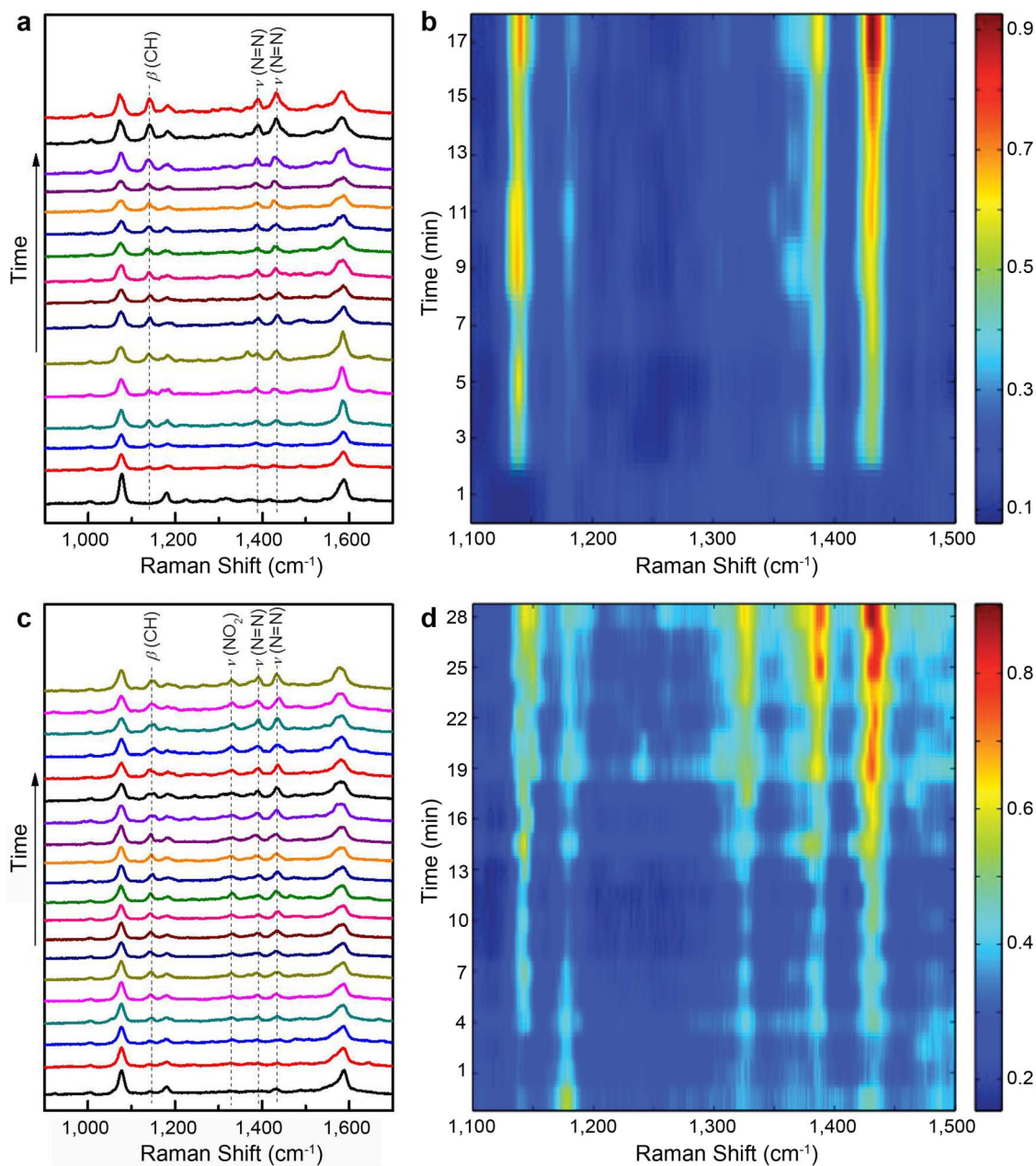


**Figure 2 | Monitoring the SPAC reaction of 4ATP in  $O_2$  atmosphere.** (a), Time-dependent SERS spectra of 4ATP under continuous 633 nm laser excitation taken every 1 min, with an integration time of 10 s and a laser power of 0.05 mW. (b), Same series as in (a), but shown as a color-coded intensity map (frequency range: 1100–1500  $cm^{-1}$ ). (c), Time-dependent SERS spectra of 4ATP under continuous 633 nm laser excitation taken every 1.5 min, with an integration time of 10 s and a laser power of 0.2 mW. (d), Same series as in (c), but shown as a color-coded intensity map (frequency range: 1100–1500  $cm^{-1}$ ).

metal surface along with the direct participation of  $O_2$  and  $H_2O$  (Fig. 3). In this mechanism,  $O_2$  acts as an electron acceptor (oxidant) while  $H_2O$  serves as a base to deprotonate the intermediates. The entire reaction is initiated by optical energy absorption (plasmonic heating<sup>20</sup>) of the 4ATP molecules bound to the metal surface, wherein they undergo electron transfer from the  $-NH_2$  groups to give  $-NH_2^+$  radical cations ( $O_2$  is an electron acceptor), which then dimerize into a diphenylhydrazine intermediate,  $Ar-NH-NH-Ar$ , following deprotonation by  $H_2O$ <sup>21,22</sup>.  $H_2O$  may also increase the local concentration of  $O_2$  at the metal surface for this oxidation reaction. A second two-electron loss and deprotonation steps lead to the formation of DMAB. Although density functional theory (DFT) calculations of the  $-NH-NH-$  group show Raman bands at frequencies distinct from the azo group (Fig. S7), the instability of the

diphenylhydrazine and its rapid conversion to DMAB prevent us from detecting this intermediate given the spectral time resolution of our experimental set-up. An alternative mechanism in pure  $O_2$  atmosphere (with relatively slower reaction rate) is also proposed to explain the SPAC conversion of 4ATP to DMAB in the absence of  $H_2O$  (Fig. S8). Under this condition,  $O_2$  acts as the electron acceptor and the intermediate superoxide ion ( $O_2^-$ ) as the deprotonation agent, where the deprotonation leads to hydroperoxyl ( $HO_2$ ) and/or hydrogen peroxide ( $H_2O_2$ ) species.  $O_2$  is a known electron acceptor; however, the deprotonation by the oxyanions ( $O_2^-$ ,  $HO_2^-$ ) may be relatively inefficient as compared to  $H_2O$ . Therefore, the reaction of 4ATP to DMAB, which involves loss of 4 electrons and 4 protons, proceeds much faster in an environment where both  $O_2$  and  $H_2O$  are present under identical optical conditions. An alternate

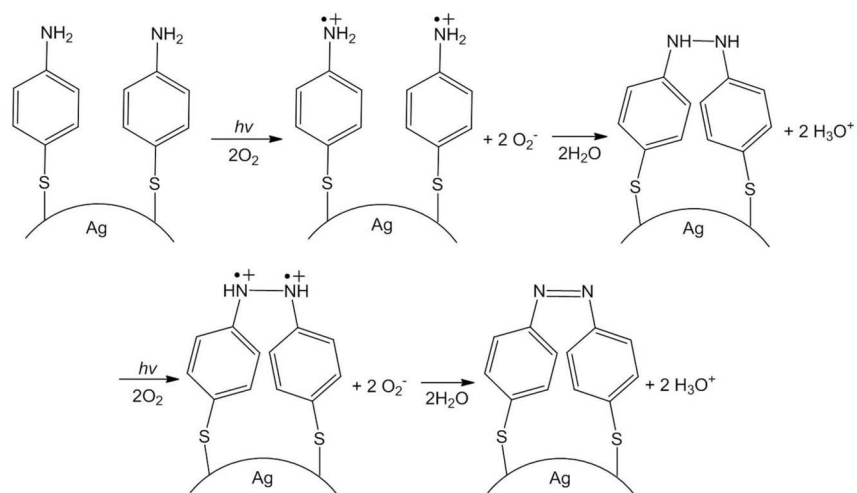


**Figure 3 | Proposed SPAC mechanism for the conversion of 4ATP to DMAB.** SPAC reaction of 4ATP dimerizing into DMAB on Ag surface under an atmosphere with both  $O_2$  and  $H_2O$  vapor. Under this condition,  $O_2$  acts as an electron acceptor, and  $H_2O$  plays the role of a deprotonation agent.

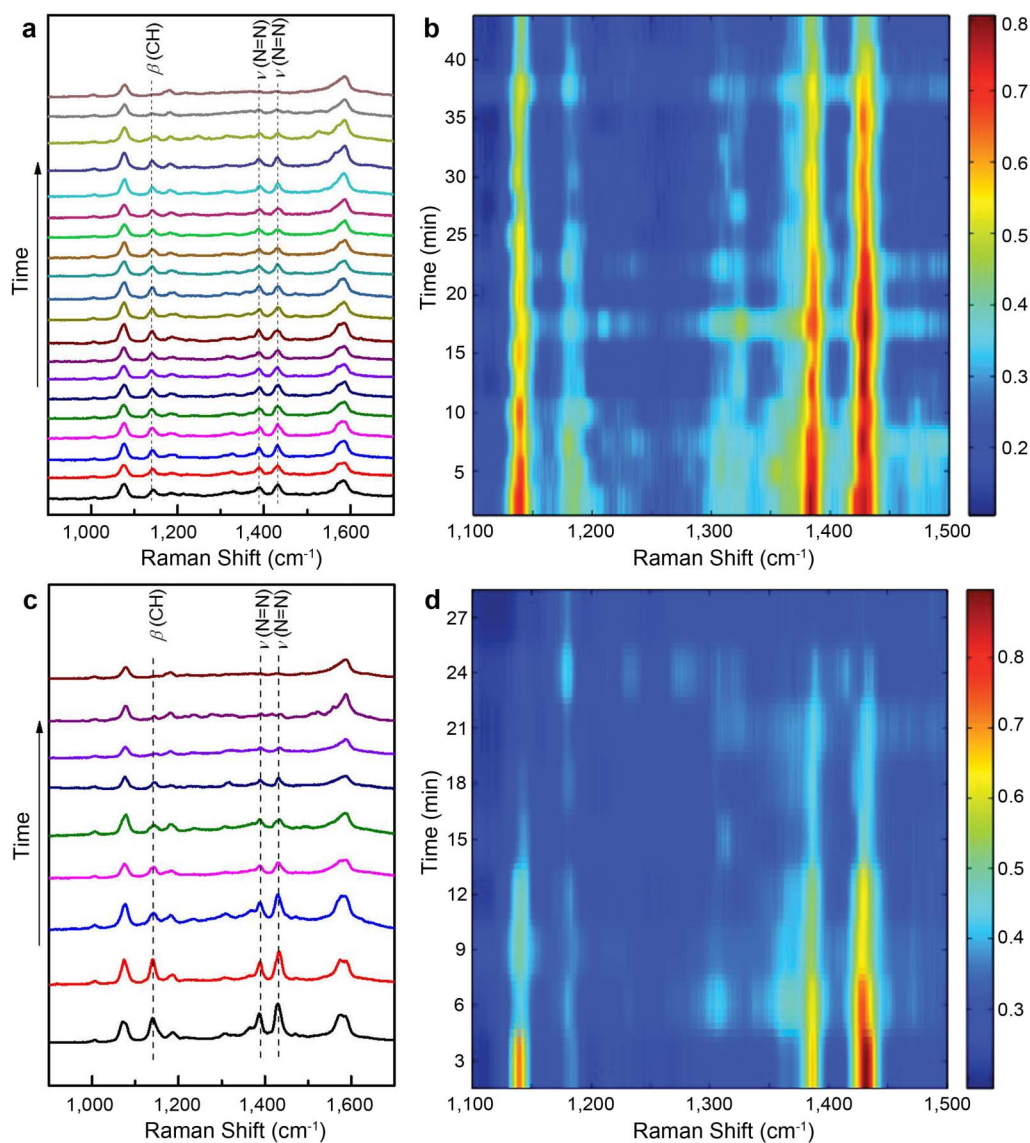


**Figure 4 | Monitoring the SPAC reaction of DMAB.** (a), Time-dependent SERS spectra of DMAB in  $H_2$  atmosphere under continuous 633 nm laser excitation taken every 2 min, with an integration time of 10 s and a laser power of 0.2 mW. (b), Same series as in (a), but shown as a color-coded intensity map (frequency range: 1100–1500  $cm^{-1}$ ). (c), Time-dependent SERS spectra of DMAB in  $N_2$  saturated  $H_2O$  atmosphere under continuous 633 nm laser excitation taken every 3 min, with an integration time of 10 s and a laser power of 0.2 mW. (d), Same series as in (c), but shown as a color-coded intensity map (frequency range: 1100–1500  $cm^{-1}$ ).



mechanism that involves nucleophilic addition of 4-ATP to 4-nitrosobenzenethiol (the latter being formed by oxidation of 4-ATP by  $O_2$  or singlet oxygen<sup>23,24</sup> in the SPAC reaction, see Fig. S9), is analogous to the oxidation of anilines in solution<sup>21,25</sup>. However, we favor the mechanism involving the hydrazine intermediate on the basis of our experimental results. Of note is that laser excitation on the bulk 4ATP cannot induce its conversion to DMAB, regardless of the applied laser wavelength and power (Fig. S10). Moreover, heat treatment of bulk 4ATP at different temperatures (60, 90, 120, and 150°C) for 30 min in air also shows no reaction occurred (Fig. S11). These results indicate the essential role of plasmon heating at the local metal surface in the conversion of 4ATP to DMAB. It has been reported that the local temperature at the gold nanoparticle surface can reach at least 408 K under 532 nm laser excitation<sup>20</sup>. In our case, we believe the local temperature at the Ag particle surface should be higher than 150°C to initiate the reaction, though the exact temperature cannot be measured by our current technique.

A recent study has observed the SPAC conversion of the reverse reaction, DMAB into 4ATP<sup>19</sup>, where water at ambient conditions was thought to be the proton source and hot electrons from surface plasmon decay were involved. Using our gas flow cell, we attempted to replicate this finding under a controlled atmosphere to better understand the mechanism of this reverse reaction, and thereby demonstrate the first complete SPAC redox cycle between 4ATP and DMAB. When DMAB is formed on the Ag surface, it can be converted back to 4ATP under a  $H_2$  atmosphere (Fig. 4 a and b), as manifested by the decrease in intensity and final disappearance of the  $\beta(CH)$  band at  $1140\text{ cm}^{-1}$  and  $\nu(N=N)$  bands at  $1390$  and  $1432\text{ cm}^{-1}$ . These DMAB Raman features remain unchanged under a  $N_2$  atmosphere, as a hydrogen source is required for the conversion from DMAB to 4ATP (Fig. S12). It should also be noted that the conversion of DMAB back to 4ATP (in the presence of  $H_2O$ ) under 633 nm laser excitation using a power of 0.05 mW proceeds very slowly (several hours), and an increase in laser power from 0.05 to 0.2 mW still requires over 40 min to complete. These long conversion times equate to dramatically slowed conversion rates as compared to the reverse reaction (4ATP to DMAB), indicating that the oxidative dimerization of the amino groups requires less energy than the reductive hydrogenation of the azo bond. In an inert atmosphere

( $N_2$ ), the reduction reaction is inhibited by the lack of a hydrogen source; however, using a  $H_2O$  saturated  $N_2$  atmosphere (Fig. 4 c and d), the reaction rate is increased by a factor of two (25 min) over using an  $H_2$  atmosphere under identical conditions, suggesting that  $H_2O$  is more efficient as a proton source than  $H_2$  gas. The details of the mechanism for the reduction of DMAB to 4ATP are not completely clear, but here we can suggest a plausible pathway. Two-electron reduction of DMAB in the presence of a proton source ( $H_2O$  or  $H_2$ ) would afford a diphenylhydrazine intermediate. Further reduction of the hydrazine intermediate would lead to N-N bond fragmentation and protonation of the resulting fragments would afford 4ATP. The source of strongly reducing equivalents needed for the reduction events (especially in the case of using  $H_2O$  as the proton source) is likely the “hot electrons” generated from surface plasmon excitation, following the reaction  $Ar-N=N-Ar + 4H_2O + 4e^- \rightarrow Ar-NH_2-NH_2-Ar + 4OH^-$ <sup>19</sup>. More interestingly, this process is entirely reversible depending on the atmosphere present; DMAB is observed again when  $O_2$  and  $H_2O$  are flowed into the reaction station. To the best of our knowledge, this is the first example demonstrating a reversible SPAC reaction, which is repeatable over many times under controlled experimental conditions. Fig. 5 shows the first 5 reversible cycles, with no obvious signal loss. It should be pointed out that conversion of 4ATP to DMAB proceeds much faster in the presence of both  $O_2$  and  $H_2O$ , as compared to its reverse reaction carried out under  $H_2$  or  $H_2O$  atmosphere under 633 nm laser excitation. This is true for 532 nm laser excitation as well; however the overall reaction rates can be accelerated.

## Discussion

Using the self-designed gas flow cell to control the reductive/oxidative atmosphere, we have conducted a mechanistic study of the SPAC reactions of 4ATP and DMAB using the SERS signal from a single Ag particle to quantify reaction products. It has been determined that SPAC conversion of 4ATP into DMAB and its reverse reaction follow different reaction mechanisms. Dimerization of 4ATP into DMAB is actually induced by efficient energy transfer (plasmonic heating) from surface plasmon resonance to the surface adsorbed 4ATP, where  $O_2$  (as an electron acceptor) is the necessary oxidant and  $H_2O$  (as a deprotonation agent) can dramatically

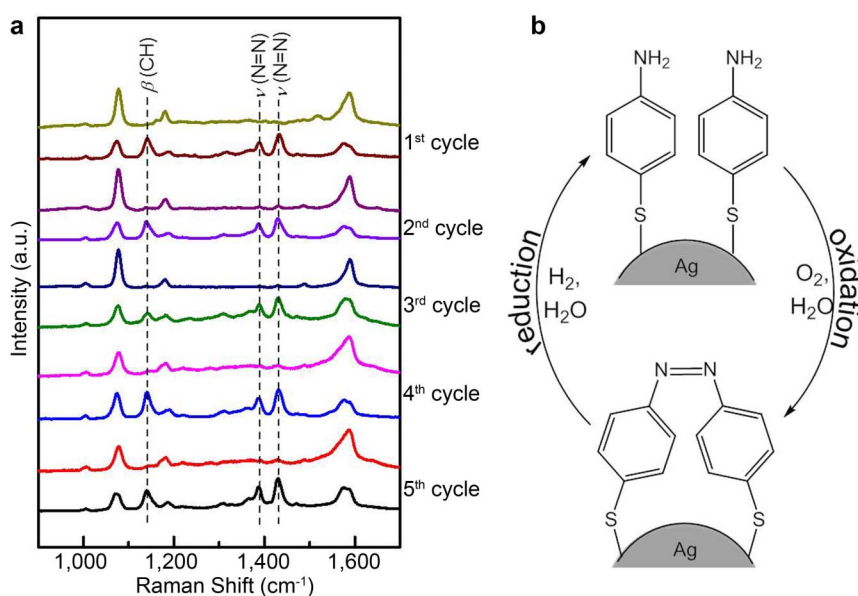


**Figure 5 | Reversibility of the 4ATP-DMAB SPAC reactions.** (a), SERS spectra were collected using 633 nm laser excitation, with an integration time of 10 s and a laser power of 0.2 mW. 4ATP was converted to DMAB by pumping  $O_2$  saturated  $H_2O$  vapor into the reaction system, and then DMAB was converted back to 4ATP by pumping  $N_2$  saturated  $H_2O$  vapor into the reaction system. (b), Schematic illustration of the reversible 4ATP-DMAB plasmonic catalytic reactions.



accelerate the reaction. However, the reverse reaction, DMAB reduced to 4ATP, results from hot electron (from surface plasmon decay) induction at the metal surface to drive the reduction (bond scission) of the azo group, where H<sub>2</sub>O or H<sub>2</sub> can act as a proton source. The reversible nature of 4ATP-DMAB conversions by surface plasmon excitation has been demonstrated as a function of their respective oxidative or reductive environments. This surface plasmon/SERS based methodology presents a unique platform to study a wide range of chemical reactions on plasmonic nanostructures that are not possible under standard synthetic conditions.

## Methods

The Ag particles used for the single particle surface enhanced Raman spectroscopy have been prepared according to previous procedures<sup>13,16</sup>. The Ag particles were immersed in 10<sup>-2</sup> mM 4ATP ethanol solution for 1 h, and then rinsed repeatedly with water and ethanol to remove any surface residuals, and then re-dispersed in ethanol to form a diluted suspension. The Ag particle suspension was then transferred to a silicon wafer, dried in air, and placed in a self-designed gas flow cell (Fig. 1). The reaction atmosphere was controlled by flowing specific gasses (N<sub>2</sub>, H<sub>2</sub>, H<sub>2</sub>O, O<sub>2</sub> or their mixtures) over the metal surface, where the SERS measurements were performed by focusing on one single Ag particle using a confocal Raman spectroscopic system (Renishaw, In Via), using 532 nm and 633 nm excitation laser and a 100× objective, with the laser spot size controlled at 2 μm in diameter.

- Lantman, E. M. V., Deckert-Gaudig, T., Mank, A. J. G., Deckert, V. & Weckhuysen, B. M. Catalytic processes monitored at the nanoscale with tip-enhanced Raman spectroscopy. *Nat Nanotechnol* **7**, 583–586 (2012).
- Huang, Y. F. *et al.* When the Signal Is Not from the Original Molecule To Be Detected: Chemical Transformation of para-Aminothiophenol on Ag during the SERS Measurement. *J Am Chem Soc* **132**, 9244–9246 (2010).
- Bailo, E. & Deckert, V. Tip-enhanced Raman scattering. *Chem Soc Rev* **37**, 921–930 (2008).
- Stiles, P. L., Dieringer, J. A., Shah, N. C. & Van Duyne, R. R. Surface-Enhanced Raman Spectroscopy. *Annu Rev Anal Chem* **1**, 601–626 (2008).
- Wu, D. Y. *et al.* Surface Catalytic Coupling Reaction of p-Mercaptoaniline Linking to Silver Nanostructures Responsible for Abnormal SERS Enhancement: A DFT Study. *J Phys Chem C* **113**, 18212–18222 (2009).
- Fang, Y. R., Li, Y. Z., Xu, H. X. & Sun, M. T. Ascertaining p,p'-Dimercaptoazobenzene Produced from p-Aminothiophenol by Selective Catalytic Coupling Reaction on Silver Nanoparticles. *Langmuir* **26**, 7737–7746 (2010).
- Huang, Y. Z., Fang, Y. R., Yang, Z. L. & Sun, M. T. Can p,p'-Dimercaptoazobisbenzene Be Produced from p-Aminothiophenol by Surface Photochemistry Reaction in the Junctions of a Ag Nanoparticle-Molecule-Ag (or Au) Film? *J Phys Chem C* **114**, 18263–18269 (2010).
- Sun, M. T., Huang, Y. Z., Xia, L. X., Chen, X. W. & Xu, H. X. The pH-Controlled Plasmon-Assisted Surface Photocatalysis Reaction of 4-Aminothiophenol to p,p'-Dimercaptoazobenzene on Au, Ag, and Cu Colloids. *J Phys Chem C* **115**, 9629–9636 (2011).
- Huang, Y. F. *et al.* Surface-enhanced Raman spectroscopic study of p-aminothiophenol. *Phys Chem Chem Phys* **14**, 8485–8497 (2012).
- Kang, L. L. *et al.* Amino Acid-Assisted Synthesis of Hierarchical Silver Microspheres for Single Particle Surface-Enhanced Raman Spectroscopy. *J Phys Chem C* **117**, 10007–10012 (2013).
- Sun, M. T. & Xu, H. X. A Novel Application of Plasmonics: Plasmon-Driven Surface-Catalyzed Reactions. *Small* **8**, 2777–2786 (2012).
- Sun, M. T., Zhang, Z. L., Zheng, H. R. & Xu, H. X. In-situ plasmon-driven chemical reactions revealed by high vacuum tip-enhanced Raman spectroscopy. *Sci. Rep.* **2**, 647; doi:10.1038/srep0064 (2012).
- Kang, L. L. *et al.* Laser wavelength- and power-dependent plasmon-driven chemical reactions monitored using single particle surface enhanced Raman spectroscopy. *Chem Commun* **49**, 3389–3391 (2013).
- Kim, K., Lee, I. & Lee, S. J. Photolytic reduction of 4-nitrobenzenethiol on Au mediated via Ag nanoparticles. *Chem Phys Lett* **377**, 201–204 (2003).
- Kim, K. *et al.* Visible laser-induced photoreduction of silver 4-nitrobenzenethiolate revealed by Raman scattering spectroscopy. *J Raman Spectrosc* **41**, 187–192 (2010).
- Zhang, B. *et al.* Acid-directed synthesis of SERS-active hierarchical assemblies of silver nanostructures. *J Mater Chem* **21**, 2495–2501 (2011).
- Dong, B., Fang, Y. R., Chen, X. W., Xu, H. X. & Sun, M. T. Substrate-, Wavelength-, and Time-Dependent Plasmon-Assisted Surface Catalysis Reaction of 4-Nitrobenzenethiol Dimerizing to p,p'-Dimercaptoazobenzene on Au, Ag, and Cu Films. *Langmuir* **27**, 10677–10682 (2011).
- Kim, K., Shin, D., Kim, K. L. & Shin, K. S. Surface-enhanced Raman scattering of 4,4'-dimercaptoazobenzene trapped in Au nanogaps. *Phys Chem Chem Phys* **14**, 4095–4100 (2012).
- Kim, K., Kim, K. L. & Shin, K. S. Photoreduction of 4,4'-Dimercaptoazobenzene on Ag Revealed by Raman Scattering Spectroscopy. *Langmuir* **29**, 183–190 (2013).
- Adleman, J. R., Boyd, D. A., Goodwin, D. G. & Psaltis, D. Heterogenous Catalysis Mediated by Plasmon Heating. *Nano Lett* **9**, 4417–4423 (2009).
- Konaka, R., Kuruma, K. & Terabe, S. Mechanisms of Oxidation of Aniline and Related Compounds in Basic Solution. *J Am Chem Soc* **90**, 1801–1806 (1968).
- Horner, L. & Dehnert, J. Azo-Aryle Und Phenazine Aus Primaren Arylaminanion Durch Autoxydation. *Chem Ber-Recl* **96**, 786–797 (1963).
- Vankayala, R., Sagadevan, A., Vijayaraghavan, P., Kuo, C. L. & Hwang, K. C. Metal Nanoparticles Sensitize the Formation of Singlet Oxygen. *Angew Chem Int Edit* **50**, 10640–10644 (2011).
- Ogilby, P. R. Singlet oxygen: there is indeed something new under the sun. *Chem Soc Rev* **39**, 3181–3209 (2010).
- Dalmagro, J., Yunes, R. A. & Simionatto, E. L. Mechanism of Reaction of Azobenzene Formation from Aniline and Nitrosobenzene in Basic Conditions - General Base Catalysis by Hydroxide Ion. *J Phys Org Chem* **7**, 399–402 (1994).

## Acknowledgements

This work was supported by NSFC (No. 21203045, 21101041, 21003029, 21071037, 91122002), Fundamental Research Funds for the Central Universities (No. HIT.NSRIF.2010065 and 2011017, and HIT.BRETH.201223), the 9<sup>th</sup> Thousand Foreign Experts Program, and Director's Postdoctoral Fellow from LANL. HLW acknowledges the financial support from the Laboratory Directed Research and Development (LDRD) fund under the auspices of DOE. Synthesis and characterization of nanostructured metals is supported by Basic Energy Science (BES), Biomolecular Materials Program, Materials Sciences and Engineering Division. PX would like to thank Prof. Mengtao Sun and Dr. Cunku Dong for the DFT calculations.

## Author contributions

L.K. and P.X. carried out the experiments and performed data processing. P.X. and N.H.M. developed the experimental set-up. P.X., X.H., K.S.S. and H.L.W. designed the experiments and proposed the mechanism. All authors contributed to the discussion of the results as well as to the writing of the manuscript.

## Additional information

**Supplementary information** accompanies this paper at <http://www.nature.com/scientificreports>

**Competing financial interests:** The authors declare no competing financial interests.

**How to cite this article:** Xu, P. *et al.* Mechanistic understanding of surface plasmon assisted catalysis on a single particle: cyclic redox of 4-aminothiophenol. *Sci. Rep.* **3**, 2997; DOI:10.1038/srep02997 (2013).



This work is licensed under a Creative Commons Attribution-NonCommercial-ShareAlike 3.0 Unported license. To view a copy of this license, visit <http://creativecommons.org/licenses/by-nc-sa/3.0>